

Recent Advances in Soot Formation from Spherical Droplet Flames at Atmospheric Pressure

C. Thomas Avedisian*
Cornell University, Ithaca, New York 14853-7501

Recent developments pertaining to the spherically symmetric combustion of sooting fuels are discussed. The spherical droplet flame is well suited for studying soot formation in droplet combustion because of the simplicity of the transport process that results from a one-dimensional combustion process. Recent advances in new experimental designs for forming and deploying droplets in a low-buoyancy environment are revealing effects that have gone unnoticed in early experimental studies. These include soot's influence on burning, the role of initial droplet diameter, and the importance of radiation. These aspects illustrate the richness of the physics and the new knowledge that continues to be forthcoming from this most basic of droplet burning configurations.

Nomenclature

B	= transfer number $\{=[QY_{O\infty}/\sigma + C_{pg}(T_{\infty} - T_d)]/h_{fg}\}$
C_{pg}	= mean gas specific heat
D	= droplet diameter
D_0	= initial droplet diameter
G	= relative acceleration ($=g/g_0$)
g	= gravitational acceleration
g_0	= Earth normal gravitational acceleration ($\approx 9.8 \text{ m/s}^2$ at the Earth's surface)
h_{fg}	= heat of vaporization of fuel
K	= burning rate for droplet combustion with convection
K_0	= burning rate for droplet combustion with no convection (spherically symmetric)
Q	= heat of combustion per unit mass of fuel
r_d	= droplet radius ($=D_0/2$)
T_d	= droplet temperature
T_{∞}	= ambient temperature
t	= time
V_{∞}	= relative velocity between droplet and ambient gas
$Y_{C_2H_2}$	= acetylene mass fraction
$Y_{O\infty}$	= oxygen mass fraction at infinity
β	= isobaric compressibility
ΔT	= $T_{\infty} - T_d$
λ_g	= mean gas thermal conductivity
ν_g	= mean gas kinematic viscosity
ρ_g	= mean gas density
ρ_l	= liquid density
σ	= stoichiometric ratio of oxygen to fuel for a single-step global reaction

I. Introduction

SOOT is the atmospheric pollution produced during the incineration of liquid hazardous wastes and the combustion of fuels within industrial scale boilers and internal-combustion (IC) engines. In these applications, soot is the dominant optically absorbing species produced during combustion of liquid fuels. Soot formation contributes to degradation of visibility, and the presence of soot agglomerates can have an impact on public health.¹ The mean soot aggregate size is very small, of the order of 10–50 nm.² Such a small

particle can easily be inhaled deep into the respiratory tract, which is a mechanism for ingestion of constituents that may be absorbed on the particles such as polycyclic aromatic hydrocarbons that are known to be mutagens, cocarcinogens, or carcinogens.³

In spite of the practical relevance of soot formation in the combustion of liquid fuels, no model of droplet combustion has included the complex pathways to forming soot. This fact is traced to the extreme complexity of soot formation. To model soot formation in droplet burning, several aspects need to be included: detailed chemistry of the oxidation process at the flame; soot nucleation, growth, and coagulation; and transport equations for soot volume fraction and number density. Radiation loss from the flame may also be important, depending on the droplet size. Because of the difficulty of modeling soot formation, the strategy in analysis is to assume the simplest transport configuration so as not to be overburdened by computing a complex velocity and temperature field as part of the problem. The spherical droplet flame is ideally suited for this purpose.

Spherically symmetric droplet combustion is characterized by a one-dimensional evaporation/flow process in which the droplet and the flame are spherical and concentric. The burning process occurs without any convection in the gas phase. It is an attractive burning condition because it removes the fluid mechanics of burning as one of the unknowns of the problem. This makes it easier to add complexities in other aspects without significant expense to computations. Concurrent to modeling, experiments are being pursued to understand spherically symmetric burning. The earliest studies date from the time of Kumagai,⁴ who was the first to study fuel droplet combustion in a buoyancy-free environment created by microgravity. A listing of the literature on experimental studies of microgravity droplet burning, including sooting and nonsooting fuels, is given by Callahan,⁵ who builds on the reviews of Yang,⁶ Jackson,⁷ and Aharon.⁸

This paper focuses on the period since the mid-1980s because experimental and numerical studies on spherically symmetric combustion of sooting fuel droplets over this period show the greatest advances. For experiments, these include using multiple spark ignition sources to promote more spherically symmetric initial conditions, observing the complete burning history of the droplet, improving photography to show the soot shell and droplet together, using smaller fibers to support droplets, and applying quantitative diagnostics to measure soot. For analyses the biggest development has been to include complex chemistry and flame radiation. The most extensive results on soot formation and its effect on droplet burning were obtained from experiments carried out at pressures of 1 atm. Experimentation on droplet combustion at high pressure in a low-convection (microgravity) environment is a considerable experimental challenge. The existing literature on high-pressure droplet

Received 29 August 1999; revision received 16 March 2000; accepted for publication 16 March 2000. Copyright © 2000 by C. Thomas Avedisian. Published by the American Institute of Aeronautics and Astronautics, Inc., with permission.

*Professor, Sibley School of Mechanical and Aerospace Engineering, Upson and Grumman Halls; cta2@cornell.edu. Associate Fellow AIAA.

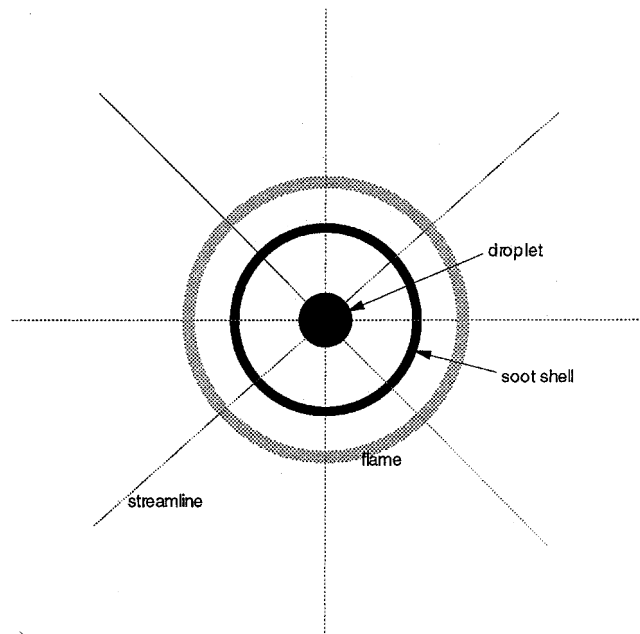
combustion does not mention soot in any significant way. A review of the high-pressure droplet combustion literature is given by Givler and Abraham.⁹

The scope of this review is as follows. First the features of sooting droplet flames and the practical importance of the problem are discussed. Then, several unique features for spherically symmetric droplet flames of sooting fuels are reviewed, followed by a discussion of experimental techniques for forming and deploying droplets in a microgravity environment to create spherical symmetry. The most commonly studied fuel is *n*-heptane, and some recent data for that fuel are presented that illustrate some of the new aspects observed in microgravity droplet studies. These include the influence of droplet diameter on burning and the role of radiation on the droplet burning process.

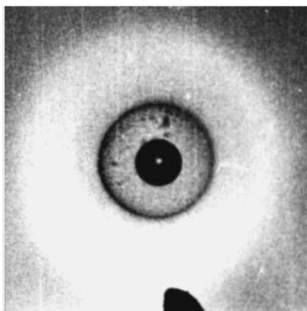
II. Features of Spherically Symmetric Sooting Droplet Flames

The obvious physical feature of a sooting spherical droplet flame is the presence of soot in the burning process. Soot precursor and aggregate particles are trapped between the droplet and the flame and form a spherical pattern or shell structure that moves in relation to the droplet and the flame diameter. Figure 1 is a schematic diagram. Soot particles are always trapped on the fuel-rich side of the flame. The shell appears in the photographic film as a dark ring that is a very porous structure.

Soot accumulation between the droplet and the flame was evident many years ago in early experiments carried out in the presence of



a)



b)

Fig. 1 a) Schematic of spherically symmetric droplet burning showing droplet, trapped soot, flame, and streamlines; b) photograph of an *n*-heptane droplet approximately 0.6 mm in diameter burning in microgravity to create a low-buoyancy environment (from Ref. 17).

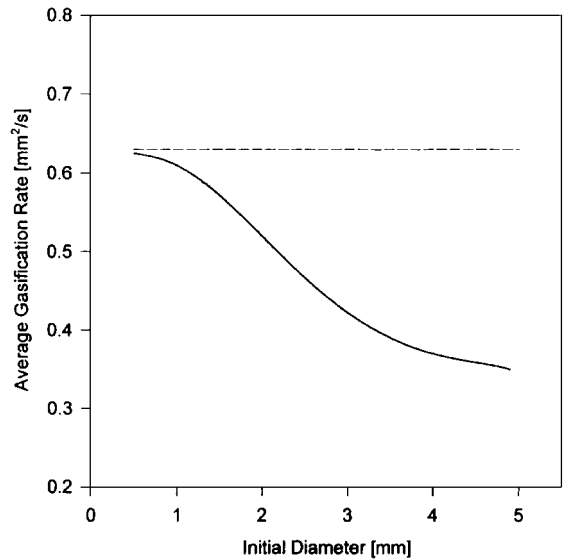


Fig. 2 Computed influence of initial droplet diameter on average burning rate for spherically symmetric methanol droplet combustion. Calculation is from Ref. 20. The solid curve includes nonluminous radiation and the dashed line neglects radiation.

strong convection (e.g., Ref. 10) and later under the condition of no convection.^{11,12} Soot was mentioned in only a perfunctory way. The mechanism by which soot particles are trapped was speculated by Knight and Williams¹³ and others^{14,15} to be due to a balance of thermophoretic and drag forces on an aggregate.

The quasi-steady approximation for spherically symmetric burning¹⁶ does not include either soot formation or radiation losses from the flame. The theory leads to the so-called *D*-squared law:

$$D^2 = D_0^2 - K_0 t \quad (1)$$

where the burning rate

$$K_0 = -8(\lambda_g / \rho_l C_{pg}) \ln(1 + B) \quad (2)$$

is found to be independent of D_0 . However, experiments clearly show that, under certain gas-phase compositions, K_0 varies with D_0 ,^{17–19} even for a nonsooting fuel like methanol.^{20,21} Within a given burning event, K_0 can also be time dependent because of the influence of D_0 on sooting and flame radiation. When K_0 is time dependent, a unique burning rate becomes an approximation for a given burning event. The conventional practice is to use data to define K_0 in a time range in which the evolution of droplet diameter is most linear. This is, of course, a significant approximation because trends of how K_0 depends on parameters like D_0 are influenced by how K_0 is defined.

Radiation heat transfer arising from soot emissions can result in both a heat gain (e.g., as measured in early studies on the problem²²) or a heat loss that is influenced by droplet diameter, as analyzed in recent studies.^{20,21,23} Although the results illustrating these processes are for only *nonsooting* flames like methanol, they illustrate trends that will be valid even for sooting spherical droplet flames. Figure 2 is a prediction from one of these studies, which illustrates how K_0 is influenced by D_0 and radiation losses for the particular case of a nonsooting methanol spherical droplet flame.²⁰ With radiation losses accounted for in the model, K_0 is lower than the no-radiation limit.

III. Relevance of Studying Single Droplets to Combustion of Droplet Clusters and Sprays

It has long been recognized²⁴ that a sound understanding of isolated droplet combustion is important for developing submodels that are used in modeling a full spray. The major characteristics of droplets in a spray are that the droplets experience strong convection and the presence of neighboring droplets. Considering an isolated droplet in a convection environment, the burning rate is

typically expressed in a power-law relationship with the Reynolds and Grashof numbers as

$$K = K_0 (1 + a Re_D^b) (1 + c Gr_D^e) \quad (3)$$

where a , b , c , and e are constants. (Regarding a droplet, the term “convective” is here taken to mean an environment in which a droplet experiences a shear force over the droplet surface that is due to a relative velocity between the droplet and surrounding gas. This force induces internal circulation within the droplet and/or asymmetries in the flame shape and flowfield. Without convection, the flowfield is purely radial and created only by evaporation of liquid at the droplet surface. The streamlines of the flow originate from the droplet surface, and are in the radial direction only as shown in Fig. 1.) There is a theoretical basis for Eq. (3) for $Gr = 0$ (Ref. 25), while Law and Williams²⁶ determined values of the constants in Eq. (3) for droplets burning from suspended fibers at atmospheric pressure. When the Grashof and Reynolds numbers approach zero, K should approach the value corresponding to spherical symmetry, K_0 . So in this sense spherically symmetric burning is a limiting condition for a droplet burning in a convection environment.

The presence of neighboring droplets in a spray complicate the droplet combustion process by the way the interdroplet distance influences gaseous diffusion and the flame shape and soot pattern. The counterpart of a spherical droplet flame is a cluster or cloud of stationary droplets, with the droplets positioned in either a random or a regular pattern, and convection is not present. Figure 3 is a schematic. The idea is for the cloud to behave like a single large droplet for moderate interdroplet spacings in which a single flame will surround the entire cloud (Fig. 3a). The flame and the soot shell are spherical because there is no convection. Adding more droplets to the cloud while keeping L_d/D fixed (assuming this were possible) expands the cloud, enlarges the flame, and proportionally more soot should form. If L_d/D is instead increased, the flame will eventually be redistributed to individual droplets, as in Fig. 1. Another analogy of sooting trends from single droplets is a moving monodispersed droplet stream (Fig. 3b). The flame and the trapped soot are shown as planar when the flame surrounds the entire stream (Figs. 3c and 3d), although in fact the flame will not be as idealized as depicted. If L_d/D increases, the flame diameter D_f decreases and proportionally less soot forms. This trend is consistent with the experiments of Kesten et al.²⁷ Increasing L_d/D is qualitatively like decreasing the diameter of a single droplet for which, as discussed below, proportionally less soot forms. The point is that varying the initial diameter of a single droplet can produce a trend in sooting tendency that has a counterpart for a stationary droplet stream or cloud. It is in this sense that single-droplet studies can provide basic insights of sooting tendencies in droplet streams or clouds.

The morphology of soot aggregates formed during spherically symmetric droplet combustion¹⁴ may not be the same as that formed in spray flames or other types of hydrocarbon flames.²⁸ However,

the mean soot aggregate size found for the spherical droplet flame, between 40 and 60 nm,¹⁴ is quite consistent with the mean aggregate size found for other types of sooting flames.² Transport conditions such as the convection patterns and temperature field surrounding the droplet do, of course, influence where aggregates are trapped, but the mean precursor size and its composition appear not to be affected by the environment.²⁹

IV. Experimental Methods

The creation of a spherically symmetric droplet burning condition is a challenge that requires removing all forms of convection while keeping the droplet stationary relative to the diagnostics that probe the flame. There are several ways to accomplish this end, all related to keeping a suitably defined Grashof (Gr) and Reynolds (Re) number small, where, $Gr_D = G g_0 \beta (T_f - T_\infty) D^3 / \nu_g^2$ and $Re = V_\infty D / \nu_g$. A common choice for the characteristic length scale for correlating experimental data is the droplet diameter.²⁶ Experiments have shown that for stationary droplets $Gr_D < 10^{-4}$ is sufficient to ensure negligible buoyancy and spherical droplet flames for atmospheric-pressure conditions.¹⁴ For the Reynolds number, values below 0.1 seem sufficient. Struk et al.³⁰ derived an alternative measure of droplet symmetry through the group $Sp \equiv \{(Pr \sqrt{Gr_f}) / [\ln(1 + Y_{O_\infty} \nu)]\}$, where the flame diameter is the characteristic length scale.

Several ways can be used to lower Sp and promote spherical symmetry: Reduce the temperature difference between the flame and ambient, lower pressure, lower D and hence D_f , and reduce gravity. Lowering pressure is counterproductive for studying soot because soot propensity decreases as pressure decreases as well as for very small droplets less than $\sim 100 \mu\text{m}$. The body of literature that shows soot shell development corresponds to $G < 10^{-4}$ for $0.4 \text{ mm} < D_0 < 5.0 \text{ mm}$.

A number of techniques have been devised for creating free-floating (unsupported) and fiber-supported droplets at low gravity. Figure 4 shows the methods involved. Some of the methods are designed to deploy droplets at $G = 1$ followed by the droplet's being placed in microgravity. Others can deploy droplets in microgravity such as in orbiting spacecraft or airplanes going through parabolic trajectories. For free-floating droplets, one technique consists of forming a droplet at the tip of two needles separated by a small distance and then rapidly withdrawing the needles at the same rate (Fig. 4a), thus leaving the droplet at the center.^{31,32} This method is designed to deploy droplets within the microgravity environment. In another technique (Fig. 4b), a droplet generator propels the test droplet in a near-vertical trajectory, and when the droplet reaches the apex of its flight, the package that houses the droplet, surrounding ambience, and the cameras is released into free fall so that all fall together.³³ This method begins at $G = 1$ and when the droplet reaches the apex of its trajectory the experiment is physically dropped to create microgravity. A similar technique that also begins

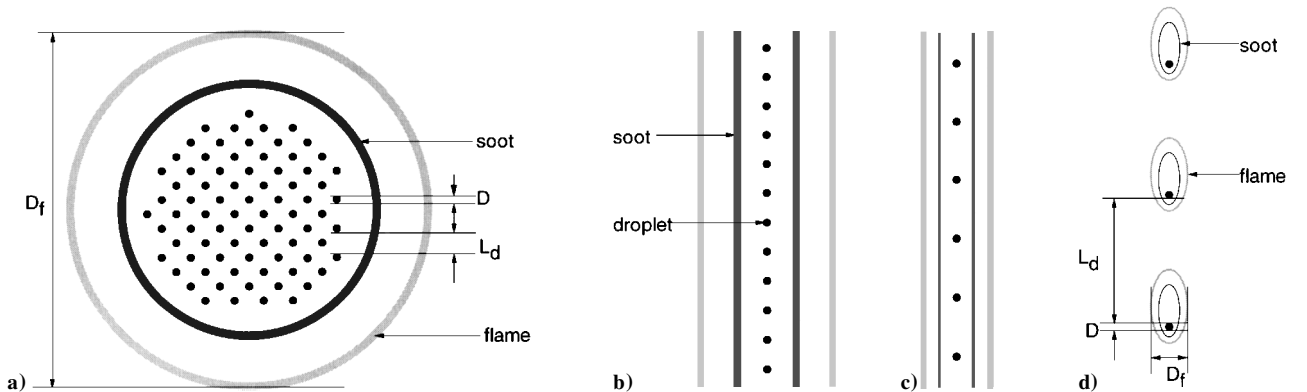
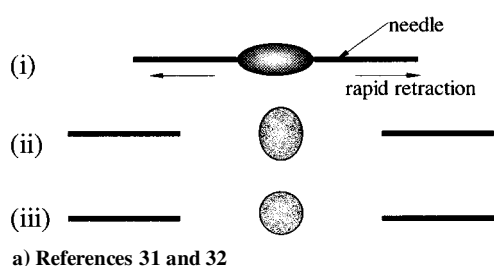
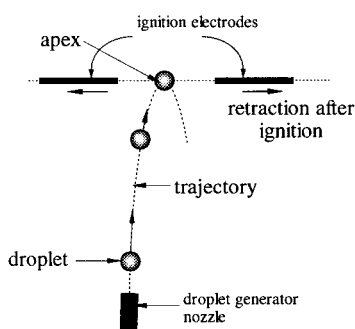


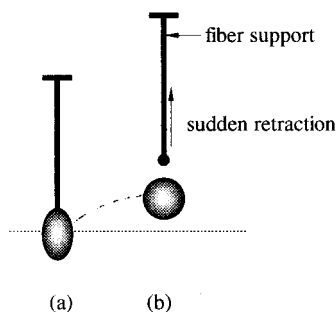
Fig. 3 a) Droplet cloud with a single large flame without convection (for very large L_d/D , flame and soot shell surround each individual droplet as in Fig. 1); b)–d) monodispersed droplet stream at various L_d/D ; flame and soot configurations are idealized as planar in b) and c). As L_d/D increases, proportionally less soot is produced.



a) References 31 and 32



b) Reference 33



c) Reference 11

Fig. 4 Experimental methods to create unsupported droplets.

at normal gravity (Fig. 4c) involves first hanging a droplet from a single fiber and then rapidly jerking the fiber to separate it from the droplet.¹¹ Like the method of Fig. 4b, when the droplet reaches the apex of its trajectory the experiment is physically dropped. For all of these methods the initial droplet diameters have ranged from 100 to 4000 μm .

Fiber-supported droplets are the easiest to use because the droplet will not move after ignition, unlike virtually all of the unsupported methods shown in Fig. 4. The only difficulty that needs to be considered is that the fiber should not be too large relative to the droplet diameter to influence the droplet shape and heat transfer through the fiber, and, of most importance to this review, the fiber should not disturb the soot pattern around the droplet.³⁴ Fiber-support methods can be used at normal and reduced gravity. The most commonly used fiber-support method is to deploy a droplet at the tip of a single fine quartz fiber with a bead at the fiber tip that is approximately twice the fiber diameter (Fig. 5b). An alternative droplet-support technique is to mount the droplet onto a lateral fiber (Fig. 5a).^{35,36} The flame would then intersect the fiber at two points on opposite sides of the droplet. For the fiber-support method, the process of placing the droplet on the fiber is challenging if the fiber diameter is significantly under 100 μm in diameter.

Ignition of the droplet is usually by spark discharge or hot wires. These two ignition methods create differing environments around the droplet at ignition. Hot wires are generally kept on for a longer period and heat the gas more extensively. Sparks are of shorter duration but can provide a considerable impulse to the droplet.³⁷ The use of two ignition sources, one on either side of the droplet, compensates for these effects and is an attempt to promote more spherically

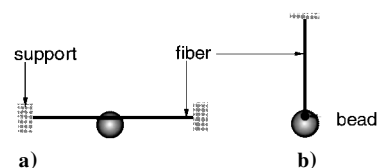


Fig. 5 Fiber-support designs used in low-gravity droplet combustion experimentation.

symmetric initial conditions. Better yet would be to use multiple ignition sources symmetrically distributed around the droplet, but even the use of two ignition sources is a considerable challenge when used in microgravity. After ignition the ignitor support rods are retracted away from the combustion zone to allow an unobstructed ambience for burning. The methods tend to be successful in creating spherical droplet flames, though internal liquid motions can arise because of the retraction process. These motions are very difficult to eliminate with any existing droplet deployment method.³⁸

The most commonly used diagnostic for analyzing the droplet burning process is photographic by a high-speed camera and/or video camera. Emulsion film is preferred for its higher feature resolution but video is easier to process. Intensified-array charge-coupled-device cameras have also proven useful for analyzing flame structure.³⁹ Using photographic information to study soot is a qualitative but certainly valid way to assess sooting tendencies if care is taken to fix the backlight intensity in comparing different burning conditions. Quantitative laser-based diagnostics are just now beginning to be applied to sooting droplet flames in microgravity. A planar laser light-scattering technique was used⁴⁰ to measure the radial distribution of scattered light intensity around pure (suspended) *n*-dodecane droplets in microgravity. The location of peak intensity was found to correlate well with measured soot shell radii.¹⁷ Light extinction with tomographic inversion was used to measure maximum soot volume fraction,^{18,41} also with success.

V. Experimental Observations

Heptane has been the most extensively studied sooting fuel for spherical droplet flames. Less extensive data have been reported on *n*-decane droplets and mixtures of heptane and hexadecane, heptane/1-monochloro-octane, and methanol and toluene. For mixtures, the liquid composition is the variable. For pure fuels, D_0 , ambient-gas composition and pressure are typically varied.

As D_0 increases, the residence time of fuel molecules between the droplet and flame also increases, which promotes more soot formation.¹⁴ As more soot forms, radiation losses increase and the conversion rate of fuel molecules is lowered, which reduces heat transfer to the droplet. If the radiation loss is excessive, the flame temperature can drop below the threshold for soot formation⁴² and a blue droplet flame will result, as observed in experiments^{30,43} for large droplets several millimeters in diameter.

Wetted porous spheres have been used to simulate the steady droplet combustion of *n*-decane, and results from the experiments showed that the flame luminosity becomes dimmer as the size of the sphere increases.³⁰ Experiments carried out in orbiting spacecraft¹⁹ showed the extinction of free-floating heptane droplets in oxygen/helium atmospheres. For droplets burning in 30% oxygen-in-helium atmospheres, the extinction of 4-mm droplets was caused by radiation losses from the flame to the ambience. For smaller droplets, extinction was believed to be caused by a conduction loss mechanism. Analysis of these results,^{20,23} including complex chemistry and radiation, showed that radiation can in fact be the cause of extinction in these oxygen/helium environments for large droplets.

The result noted above, that K_0 is dependent on D_0 for the spherically symmetric burning of a sooting fuel^{14,17,18} is traceable to radiation loss from the flame and soot formation. Larger droplets burn more slowly than smaller droplets, and quantitative measurements of soot volume fraction with D_0 show that proportionally more soot is formed as D_0 increases,^{18,41} which is consistent with the residence

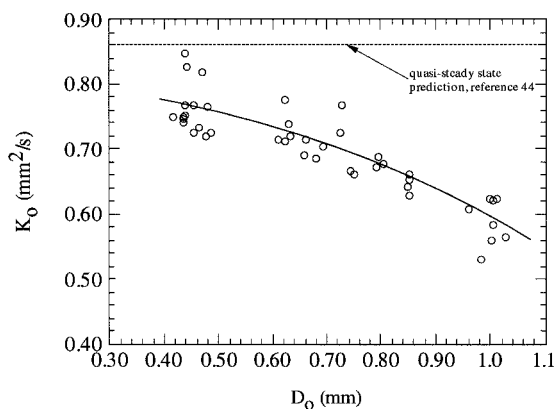


Fig. 6 Measured *n*-heptane burning rates for the initial droplet diameters shown. Data are from Ref. 17. The curve is drawn to suggest a trend. The prediction is from the complex chemistry model of Ref. 44, which does not include radiation losses.

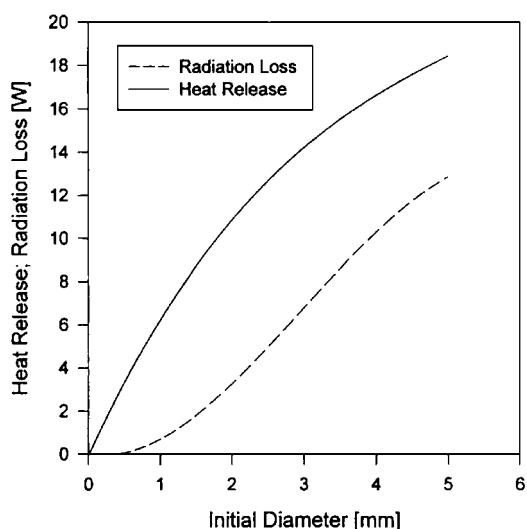


Fig. 7 Calculation²¹ comparing the chemical energy release with radiative heat loss at one instant of time ($tK_0/D_0^2 = 0.40$) and a range of initial droplet diameters for spherically symmetric methanol droplet combustion.

time being proportional to D_0^2 (Ref. 14). Figure 6 is a crossplot of K_0 with D_0 for heptane¹⁷ that shows this effect in the range of D_0 given (the dashed line is from a numerical simulation⁴⁴). This trend was also predicted for methanol, which does not produce soot. Nonluminous flame radiation, as distinct from luminous radiation from soot, is therefore also an effective heat loss mechanism that increases as D_0 increases. Radiation, as distinct from soot formation, is an independent mechanism to influence heat transport to the droplet. Figure 7 is a prediction²¹ that shows that when D_0 is increased the radiative loss for methanol becomes comparable with the chemical heat release. Below 0.5 mm, the influence of radiation is negligible and the burning rate approaches the no-radiation limit. This trend is further illustrated in Fig. 2 for methanol droplets computed from two models; one including radiation and the other neglecting it. For droplets below ~ 0.5 mm in diameter, radiation has no influence on burning.

Measurements of the maximum soot volume fraction (f_v) in heptane spherical droplet flames¹⁸ show that f_v decreases as the initial droplet diameter increases. Figure 8 illustrates this trend for heptane droplets for $0.8 \text{ mm} < D_0 < 2 \text{ mm}$. The relatively low volume fractions measured may indicate that the soot shell is not an effective physical barrier to influence molecular transport.

As noted above, radiation heat losses from the flame can lower the flame temperature to a point at which combustion ceases and extinction is predicted.^{21,23,30,45–47} Limited experiments have shown

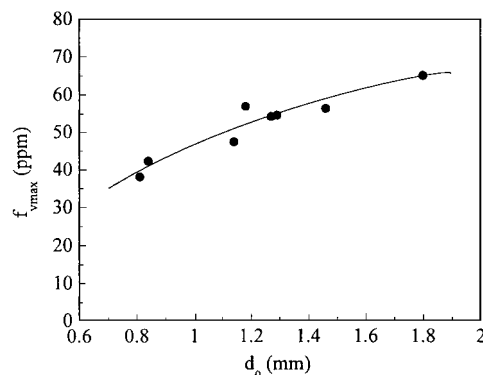


Fig. 8 Variation of maximum soot volume fraction with initial droplet diameter measured by Lee et al.¹⁸ around fiber-supported (see Fig. 5a) *n*-heptane droplets burning in atmospheric air in a drop tower to create microgravity and promote spherical symmetry. The curve is drawn to suggest the trend.

this form of radiative extinction for large *n*-heptane droplets of several millimeters in diameter.^{19,30} There is a delay time after ignition before soot forms. The delay time is shown to agree with the estimated time of carbonization of precursor particles.²⁸ In this period the flame color appears blue, as observed for heptane droplets several millimeters in diameter.⁴³

Most of the experimental evidence shows the burning rate continually decreasing as the droplet diameter increases. Exceptions are usually attributed to low residual levels of convection.^{19,43,48} The measurements of Hara and Kumagai^{32,49} show that K_0 increases with D_0 for heptane burning in air for $D_0 < 1.0 \text{ mm}$, and Nayagam et al.¹⁹ show similar trends for heptane burning in 25% oxygen/helium atmospheres for $D_0 > 2.5 \text{ mm}$. Note that, from Eq. (2), K_0 increases as D increases for burning with convection. The relation between K and D_0 is even more complex if K_0 depends on droplet diameter.

Other parameters in addition to D_0 affect sooting. Increasing pressure should increase sooting propensity. If increased soot formation leads to reduced heat transfer to the droplet, then K_0 should decrease as pressure increases. Such a trend is consistent with results reported by Choi et al.¹⁵ for pressure levels between sub-atmospheric and atmospheric. At higher pressures, K_0 increases as pressure increases.^{50,51} As pressure increases the heat of vaporization decreases (it is zero at a liquid's critical point) and fuel vaporization increases, which both act in favor of increasing the burning rate to override an influence of increased sooting. Soot shells were not observed at high pressure,^{50,51} possibly because of excessive convection levels.

The preceding discussion focused on single-component fuels. For mixtures, composition introduces another complication to soot formation. Few studies have experimentally examined sooting mixture droplets in microgravity. Mixtures of heptane and hexadecane,^{8,38,43,52,53} methanol/toluene,⁵⁴ heptane and 1-monochlorooctane,¹⁴ and an emulsion of water-in-heptane⁵⁵ have been examined. As expected, the effect of composition is most dramatic for mixtures with components that have large differences in their sooting propensities. A good example is methanol and toluene. For this mixture, methanol dilution has a strong effect on soot shell image intensity, and from that we infer soot formation. Similar trends have been shown for water-in-heptane emulsions,⁵⁵ in which the combustion process was shown to be well represented by the frozen limit process.⁵⁶

VI. Modeling Soot Formation in Spherically Symmetric Droplet Flames

Throughout this paper, results from various models of spherically symmetric droplet combustion were mentioned.^{20,21,23,45} These studies were used to explain experimental trends from spherical sooting droplet flames. The analyses of the past 10 years or so significantly extended the basic quasi-steady assumptions of the

D-squared law by incorporating flame radiation, complex chemistry, and transient gas-phase processes. Calculations of how D_0 influences flame radiation and burning rate showed trends consistent with measurements, but the comparisons are not quantitative because the most advanced models still do not include soot formation itself. This fact places a high reliance on experimental observations in the meantime, and data will be needed to validate any model of a sooting fuel droplet.

Complex chemistry was first included in a droplet model by Cho et al.⁵⁷ for methanol—a nonsooting fuel. Zhang et al.⁵⁸ used a reduced chemistry model to analyze flame chemistry. Jackson and Avedisian⁴⁴ used the complex chemistry scheme of Warnatz⁵⁹ and a quasi-steady assumption to model heptane droplet burning, whereas Cho and Dryer⁶⁰ used the same mechanism and also assumed unsteady gas phase transport. Marchese et al.²³ adapted a refined reaction scheme for heptane and transient gas- and liquid-phase processes to droplet combustion. They also added nonluminous radiation to the model. The Warnatz⁵⁹ scheme was compared and differences were substantial for acetylene concentration but both yielded essentially the same gas temperature profile and quasi-steady burning rates.

Analysis of the trapping mechanism for soot aggregates was incorporated in a quasi-steady model with complex chemistry⁴⁴ that used the Warnatz⁵⁹ mechanism and a model of soot aggregates as being essentially particles of various sizes in the flow that did not affect transport. The results showed decreased stability of trapping as aggregate size increased. It is speculated²⁸ that in the early stage of formation the shell is composed of soot precursor particles. The particles are formed after a delay time. At later times, when carbonization of precursor particles increases their size, the larger soot globules become less solidly trapped in the shell because of reduced forces on them (from drag and thermophoresis) that scale with the particle size.⁴⁴ Any small perturbation in the spherical symmetry can cause the shell to break up and result in aggregates drifting outward toward the flame. This decreased shell stability as burning progresses is consistent with experimental observations that show large aggregates moving through the flame late in the burning process.¹⁷

One of the byproducts of including complex chemistry is the ability to compute concentrations of combustion products that are soot precursor species. Acetylene (C_2H_2) is a major soot precursor species,¹⁶ and soot formation should be traceable to the amount of acetylene produced. The reaction mechanisms of Warnatz⁵⁹ and Marchese et al.²³ for heptane predict different quantitative amounts of acetylene formed, although, as noted above, they predict essentially the same gas-phase temperature distribution. We will assume that general trends of how acetylene varies with parameters like D_0 are not going to be substantially different among different reaction schemes. The only study that predicted how C_2H_2 varies with D_0 is from Jackson and Avedisian⁴⁴ which neglected radia-

tion for the Warnatz⁵⁹ scheme. The total amount of acetylene is integrated between the droplet surface and far ambience (which we take as m_{soot}) and is divided by the mass of fuel evaporated, m_{fuel} ; Fig. 9 shows how $m_{\text{soot}}/m_{\text{fuel}}$ varies with droplet radius ($r_d = D_0/2$ in Fig. 9). The increase in acetylene concentration relative to fuel evaporation should translate to increased soot formation and thus an increase in soot volume fraction as diameter increases. Such a trend is qualitatively consistent with measurements of soot volume fraction with diameter, as shown in Fig. 8 for heptane droplets with $D_0 < 2$ mm (Ref. 18). Unfortunately, we cannot be more quantitative on the mechanism of how D_0 influences soot formation. Also, no measurements have been made on the distribution of gaseous species surrounding a sooting fuel droplet burning in microgravity to promote spherically symmetric burning. A more comprehensive model of soot formation for spherically symmetric droplet burning conditions will be required, which is the challenge for the future.

VII. Conclusions

New knowledge about the role and importance of soot formation is being obtained by a study of the spherically symmetric droplet combustion process. This fact is due to improved experimental designs and quantitative diagnostics applied to the problem. The ability to predict soot formation and its effect on spherically symmetric droplet burning has not been accomplished, and it remains as one of the outstanding problems for this most basic of droplet burning configurations. The recent experimental evidence reviewed here shows that the influence of soot formation and flame radiation increases as the initial droplet diameter increases. Numerical modeling of nonluminous spherically symmetric droplet burning, which includes nonluminous radiation, shows that there is a threshold to droplet diameter below which radiation losses are not important. For this small droplet diameter range, it is justifiable to neglect radiation. Measurements of soot volume fraction from spherical *n*-heptane droplet flames show that volume fraction increases with increasing initial droplet diameter for $D_0 < 2$ mm.

The challenge for the future is twofold: develop a comprehensive model of spherically symmetric droplet burning that includes soot formation (i.e., pyrolysis reactions, formation of soot precursors, their growth by oxidation, and the rates of the steps involved); and continue to improve data quality with improved experimental designs for burning of stationary droplets in a low convection environment.

Acknowledgments

The author is pleased to acknowledge financial support from the National Aeronautics and Space Administration, Grant NAG-1791 and NAG3-2224 (M. K. King, Program Director; D. L. Dietrich, Project Monitor), in preparation of this manuscript. Thanks also go to Tony Webber and Tomo Wiggins for help with the manuscript.

References

- Howard, J. B., and Kausch, W. J., "Soot Control by Fuel Additives," *Progress in Energy and Combustion Science*, Vol. 6, 1980, pp. 263–276.
- Megaridis, C. M., and Dobbins, R. A., "Comparison of Soot Growth and Oxidation in Smoking and Non-Smoking Ethylene Diffusion Flames," *Combustion Science Technology*, Vol. 66, 1989, pp. 1–16.
- Barfknecht, T. R., "Toxicology of Soot," *Progress in Energy and Combustion Science*, Vol. 9, 1983, pp. 199–237.
- Kumagai, S., "Combustion of Fuel Droplets in a Falling Chamber with Special Reference to the Effect of Natural Convection," *Jet Propulsion*, Vol. 26, 1956, p. 786.
- Callahan, B. J., "Droplet Combustion of Nonane, Hexanol and Their Mixtures in Reduced Gravity," M.S. Thesis, Cornell Univ., Ithaca, NY, 2000.
- Yang, J. C., "An Experimental Method for Studying Combustion of an Unsupported Fuel Droplet at Reduced Gravity," Ph.D. Dissertation, Cornell Univ., Ithaca, NY, 1990.
- Jackson, G. S., "Spherically Symmetric Droplet Combustion of Sooting and Multi-component Fuels," Ph.D. Dissertation, Cornell Univ., Ithaca, NY, 1994.
- Aharon, I., "Theoretical and Experimental Studies on Evaporation and Combustion of Multicomponent Droplets in Reduced Gravity," Ph.D. Dissertation, Univ. of California, Davis, CA, 1996.

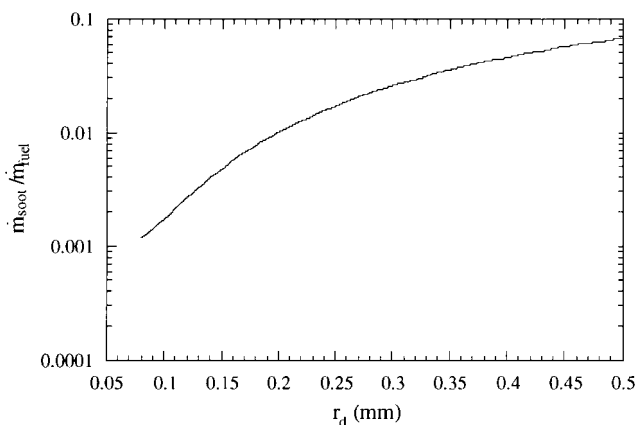


Fig. 9 Predicted variation of relative acetylene concentration with initial droplet radius ($r_d = D_0/2$) for *n*-heptane droplet combustion (from Ref. 44).

- ⁹Givler, S. D., and Abraham, J., "Supercritical Droplet Vaporization and Combustion Studies," *Progress in Energy and Combustion Science*, Vol. 22, 1996, pp. 1–28.
- ¹⁰Kobayashi, H., "An Experimental Study on the Combustion of a Fuel Droplet," *5th Symposium (International) on Combustion*, The Combustion Inst., Pittsburgh, PA, 1955, pp. 141–148.
- ¹¹Okajima, S., and Kumagai, S., "Further Investigations of Combustion of Free Droplets in a Freely Falling Chamber including Moving Droplet," *15th Symposium (International) on Combustion*, The Combustion Inst., Pittsburgh, PA, 1975, pp. 401–407.
- ¹²Okajima, S., and Kumagai, S., "Experimental Studies on Combustion of Moving and Stationary Free Droplets Under Zero Gravity," *Archivum Termodynamiki i Spalania*, Vol. 7, 1976, pp. 41–55.
- ¹³Knight, B., and Williams, F. A., "Observations on the Burning of Droplets in the Absence of Buoyancy," *Combustion and Flame*, Vol. 38, 1980, pp. 111–119.
- ¹⁴Jackson, G. S., Avedisian, C. T., and Yang, J. C., "Observations of Soot During Droplet Combustion at Low Gravity: Heptane and Heptane/Monochloroalkane Mixtures," *International Journal of Heat and Mass Transfer*, Vol. 35, No. 8, 1992, pp. 2017–2033.
- ¹⁵Choi, M. Y., Dryer, F. L., Green, G. J., and Sangiovanni, J. J., "Soot Agglomeration in Isolated, Free Droplet Combustion," AIAA Paper 93-0823, Jan. 1993.
- ¹⁶Glassman, I., *Combustion*, 2nd ed., Harcourt Brace Jovanovich, Orlando, FL, 1987.
- ¹⁷Jackson, G. S., and Avedisian, C. T., "The Effect of Initial Diameter in Spherically Symmetric Droplet Combustion of Sooting Fuels," *Proceedings of the Royal Society London A*, Vol. 446, 1994, pp. 255–276.
- ¹⁸Lee, O. L., Manzello, S. L., and Choi, M. Y., "The Effects of Initial Diameter on Sooting and Burning Behavior of Isolated Droplets Under Microgravity Conditions," *Combustion Science and Technology*, Vol. 132, 1998, pp. 139–156.
- ¹⁹Nayagam, V., Haggard, J. B., Colantonio, R. O., Marchese, A. J., Dryer, F. L., Zhang, B. L., and Williams, F. A., "Microgravity *n*-Heptane Droplet Combustion in Oxygen–Helium Mixtures at Atmospheric Pressure," *AIAA Journal*, Vol. 56, 1998, pp. 1369–1378.
- ²⁰Marchese, A. J., Dryer, F. L., and Colantonio, R. O., "Radiative Effects in Space-Based Methanol/Water Droplet Combustion Experiments," *27th Symposium (International) on Combustion*, The Combustion Inst., Pittsburgh, PA, 1998, pp. 2627–2634.
- ²¹Marchese, A. J., and Dryer, F. L., "The Effect of Non-Luminous Thermal Radiation in Microgravity Droplet Combustion," *Combustion Science and Technology*, Vol. 124, 1997, pp. 371–402.
- ²²Hottel, H. C., Williams, G. C., and Simpson, H. C., "Combustion of Heavy Liquid Fuels," *5th Symposium (International) on Combustion*, The Combustion Inst., Pittsburgh, PA, 1955, pp. 101–129.
- ²³Marchese, A. J., Dryer, F. L., and Nayagam, V., "Numerical Modeling of Isolated *n*-Alkane Droplet Flames: Initial Comparisons with Ground and Space-Based Microgravity Experiments," *Combustion and Flame*, Vol. 116, 1998, pp. 432–459.
- ²⁴Sirignano, W. A., "Fuel Vaporization and Spray Combustion Theory," *Progress in Energy and Combustion Science*, Vol. 9, 1983, pp. 291–322.
- ²⁵Gogos, G., Sadhal, S. S., Ayyaswamy, P. S., and Sundarajan, T., "Thin Flame Theory for the Combustion of a Moving Liquid Droplet: Effects Due to Variable Density," *Journal of Fluid Mechanics*, Vol. 171, 1986, pp. 121–144.
- ²⁶Law, C. K., and Williams, F. A., "Kinetics and Convection in the Combustion of Alkane Droplets," *Combustion and Flame*, Vol. 19, 1972, pp. 393–405.
- ²⁷Kesten, A. S., Sangiovanni, J. J., and Goldberg, P., "Conceptual Examination of Gas Phase Particulate Formation in Gas Turbine Combustors," *Journal of Engineering for Power*, Vol. 102, 1980, pp. 613–618.
- ²⁸Dobbins, R. A., Govatzidakis, G. J., Lu, W., Schwartzman, A. F., and Fletcher, R. A., "Carbonization Rate of Soot Precursor Particles," *Combustion Science and Technology*, Vol. 121, 1996, pp. 103–121.
- ²⁹Dobbins, R. A., Fletcher, R. A., and Chang, H. C., "The Evolution of Soot Precursor Particles in a Diffusion Flame," *Combustion and Flame*, Vol. 115, 1998, pp. 285–298.
- ³⁰Struk, P. M., Dietrich, D. L., and T'ien, J. S., "Large Droplet Combustion Experiment Using Porous Spheres Conducted in Reduced Gravity Aboard an Aircraft-Extinction and the Effects of *g*-Jitter," *Microgravity Science and Technology*, Vol. 9, No. 2, 1996, pp. 106–116.
- ³¹Haggard, J. B., and Kropp, J. L., "Droplet Combustion Drop Tower Tests Using Models of the Space Flight Apparatus," AIAA Paper 87-0576, Jan. 1987.
- ³²Hara, H., and Kumagai, S., "The Effect of Initial Diameter on Free Droplet Combustion with Spherical Flame," *25th Symposium (International) on Combustion*, The Combustion Inst., Pittsburgh, PA, 1994, pp. 423–430.
- ³³Avedisian, C. T., Yang, J. C., and Wang, C. H., "On Low Gravity Droplet Combustion," *Proceedings of the Royal Society of London A*, Vol. 420, 1988, pp. 183–200.
- ³⁴Avedisian, C. T., and Jackson, G. S., "Soot Patterns Around Suspended *n*-Heptane Droplet Flames in a Convection-Free Environment" (to be published).
- ³⁵Lebedev, O. N., and Marchenko, V. N., "An Experimental Study of Vaporization of Droplets of Hydrocarbon Fuels at High Gas Temperatures and Pressures," *Heat Transfer–Soviet Research*, Vol. 11, No. 3, 1979, pp. 92–98.
- ³⁶Dietrich, D. L., and Haggard, J. B., "Combustion of Interacting Droplet Arrays in a Microgravity Environment," NASA Conf. Publ. 10113, 1992, pp. 317–323.
- ³⁷Shaw, B. D., Dryer, F. L., Williams, F. A., and Gat, N., "Interactions Between Gaseous Electrical Discharges and Single Liquid Droplets," *Combustion and Flame*, Vol. 74, 1988, pp. 233–254.
- ³⁸Shaw, B. D., and Chen, A. G., "Observation of Flows Inside Droplets Undergoing Combustion in Reduced Gravity," *Microgravity Science and Technology*, Vol. 10, No. 3, 1997, pp. 136–143.
- ³⁹Marchese, A. J., Dryer, F. L., Nayagam, V., and Colantonio, R. O., "Hydroxyl Radical Chemiluminescence Imaging and the Structure of Microgravity Droplet Flames," *26th Symposium (International) on Combustion*, The Combustion Inst., Pittsburgh, PA, 1996, pp. 1219–1226.
- ⁴⁰Tuse, M., Segawa, D., Kadota, T., and Yamasaki, H., "Observation of Sooting Behavior in an Emulsion Droplet Flame by Planar Laser Light Scattering in Microgravity," *26th Symposium (International) on Combustion*, The Combustion Inst., Pittsburgh, PA, 1996, pp. 1251–1258.
- ⁴¹Choi, M. Y., and Lee, K. O., "Investigation of Sooting in Microgravity Droplet Combustion," *26th Symposium (International) on Combustion*, The Combustion Inst., Pittsburgh, PA, 1996, pp. 1243–1249.
- ⁴²Gomez, A., Littman, M. G., and Glassman, I., "Comparative Study of Soot Formation on the Centerline of Axisymmetric Laminar Diffusion Flames: Fuel Temperature Effects," *Combustion and Flame*, Vol. 70, 1987, pp. 225–241.
- ⁴³Dietrich, D. L., Haggard, J. B., Dryer, F. L., Nayagam, V., Shaw, B. D., and Williams, F. A., "Droplet Combustion Experiments in Space-lab," *26th Symposium (International) on Combustion*, The Combustion Inst., Pittsburgh, PA, 1996, pp. 1201–1207.
- ⁴⁴Jackson, G. S., and Avedisian, C. T., "Modeling of Spherically Symmetric Droplet Flames Including Complex Chemistry: Effect of Water Addition on *n*-Heptane Droplet Combustion," *Combustion Science and Technology*, Vol. 115, 1996, pp. 127–147.
- ⁴⁵Marchese, A. J., and Dryer, F. L., "The Effect of Liquid Mass Transport on the Combustion and Extinction of Bicomponent Droplets of Methanol and Water," *Combustion and Flame*, Vol. 105, 1996, pp. 104–122.
- ⁴⁶Chao, B. H., Law, C. K., and T'ien, J. S., "Structure and Extinction of Diffusion Flames with Flame Radiation," *23rd Symposium (International) on Combustion*, The Combustion Inst., Pittsburgh, PA, 1990, pp. 523–531.
- ⁴⁷Mills, K., and Matalon, M., "Extinction of Spherical Diffusion Flames in the Presence of Radiant Loss," *27th Symposium (International) on Combustion*, The Combustion Inst., Pittsburgh, PA, 1996, pp. 2535–2541.
- ⁴⁸Choi, M. Y., Dryer, F. L., and Haggard, J. B., "Observations on a Slow Burning Regime of Hydrocarbon Droplets: *n*-Heptane/Air Results," *23rd Symposium (International) on Combustion*, The Combustion Inst., Pittsburgh, PA, 1990, pp. 1597–1604.
- ⁴⁹Hara, H., and Kumagai, S., "Experimental Investigation of Free Droplet Combustion Under Microgravity," *23rd Symposium (International) on Combustion*, The Combustion Inst., Pittsburgh, PA, 1990, pp. 1605–1611.
- ⁵⁰Sato, J., Tsue, M., Niwa, M., and Kono, M., "Effects of Natural Convection on High-Pressure Droplet Combustion," *Combustion and Flame*, Vol. 82, 1990, pp. 142–150.
- ⁵¹Chaveau, C., Chesneau, X., and Gökalp, I., "Burning Characteristics of *n*-Heptane Droplets Under Different Regimes," AIAA Paper 93-0824, Jan. 1993.
- ⁵²Yang, J. C., and Avedisian, C. T., "The Combustion of Unsupported Heptane/Hexadecane Mixture Droplets at Low Gravity," *22nd Symposium (International) on Combustion*, The Combustion Inst., Pittsburgh, PA, 1988, pp. 2037–2044.
- ⁵³Aharon, I., and Shaw, B. D., "Estimates of Liquid Species Diffusivities from Experiments on Reduced-Gravity Combustion of Heptane–Hexadecane Droplets," *Combustion and Flame*, Vol. 113, 1998, pp. 507–518.
- ⁵⁴Jackson, G. S., Avedisian, C. T., and Yang, J. C., "Soot Formation During Combustion of Unsupported Methanol/Toluene Mixture Droplets in Microgravity," *Proceedings of the Royal Society of London A*, Vol. 435, 1991, pp. 359–369.

⁵⁵Jackson, G. S., and Avedisian, C. T., "Combustion of Unsupported Water-in-Heptane Emulsion Droplets in a Convection-Free Environment," *International Journal of Heat and Mass Transfer*, Vol. 41, No. 16, 1998, pp. 2503–2515.

⁵⁶Law, C. K., Lee, C. H., and Srinivasan, N., "Combustion Characteristics of Water-in-Oil Emulsion Droplets," *Combustion and Flame*, Vol. 37, 1980, pp. 125–143.

⁵⁷Cho, S. Y., Yetter, R. A., and Dryer, F. L., "A Computer Model for One-Dimensional Mass and Energy Transport in and Around Chemically Reacting Particles, Including Complex Gas-Phase Chemistry, Multicomponent

Molecular Diffusion, Surface Exploration, and Heterogeneous Reaction," *Journal of Computational Physics*, Vol. 102, 1992, pp. 160–179.

⁵⁸Zhang, B. L., Card, J. M., and Williams, F. A., "Application of Rate-Ratio Asymptotics to the Prediction of Extinction for Methanol Droplet Combustion," *Combustion and Flame*, Vol. 105, 1996, pp. 267–290.

⁵⁹Warnatz, J., *Combustion Chemistry* edited by W. C. Gardner, Jr., Springer-Verlag, New York, 1984, Chap. 5.

⁶⁰Cho, S. Y., and Dryer, F. L., "A Numerical Study of the Unsteady Burning Behavior of *n*-Heptane Droplets," *Combustion Theory and Modeling*, Vol. 3, 1999, pp. 67–280.